VIII International Conference on Computational Plasticity
COMPLAS VIII
E. Oñate and D.R.J. Owen (Eds)

THE MECHANICAL RESPONSE OF A CERAMIC POLYCRYSTALLINE MATERIAL WITH INTER-GRANULAR LAYERS

Eligiusz W. Postek⋆, Tomasz Sadowski†, and Stephen J. Hardy⋆

⋆School of Engineering
University of Wales Swansea
Singleton Park, SA2 8PP Swansea, Wales, United Kingdom
e-mail: e.w.postek,s.j.hardy@swansea.ac.uk, web page: http://www.swansea.ac.uk

†Faculty of Civil and Sanitary Engineering
Lublin University of Technology
ul. Nabystrzycka 40, 20-618 Lublin, Poland
e-mail: sadowski@akropolis.pol.lublin.pl, web page:
http://akropolis.pol.lublin.pl/users/sadowski/index.htm

Key words: Ceramics, Interfaces, Finite Strains.

Summary. *This paper describes an investigation into the behaviour of a two-phase ceramic polycrystalline composite material. Observations of SME images show that the polycrystals consist of grains and relatively thin intergranular layers. The properties of the layers can significantly affect the behaviour of the entire polycrystal. The grains may be elastic and the layers can be metallic as in this case.*

1 INTRODUCTION

A typical application of polycrystalline materials is the fabrication of cutting tools. The tools are working in such severe conditions as high dynamic and temperature loadings. An exemplary two-phase material used for them may consist of elastic grains and ductile interfaces. The interfaces are thick enough not to be treated as only contacting adhesive layers. Our interest will focus on the behavior of the relatively thick intergranular layers which affect performance of entire sample. An example of SME image showing grains, interfaces and their ideogramic idealization are presented in Figure 1 (left, middle). The grains can exhibit anisotropic behaviour.

2 FORMULATION

The incremental linearized and FE discretized form of the nonlinear equation of equilibrium fulfilling boundary and initial conditions valid for elasto-plastic problem with nonlinear geometry[1,2,3,4] is given below

$$\left(\int\limits_{\Omega^t} \mathbf{B}_{\mathrm{L}}^{\prime \mathrm{T}} {}_t^t\bar{\boldsymbol{\tau}} \mathbf{B}_{\mathrm{L}}^{\prime} \, d\Omega^t \right) \Delta\mathbf{q} + \int\limits_{\Omega^t} \mathbf{B}_{\mathrm{L}}^{\mathrm{T}} \Delta\mathbf{S} \, d\Omega^t = \int\limits_{\Omega^t} \mathbf{N}^{\mathrm{T}} \Delta\mathbf{f} \, d\Omega^t + \int\limits_{\partial\Omega^t} \mathbf{N}^{\mathrm{T}} \Delta\mathbf{t} \, \left(\partial\Omega_\sigma^t\right) \qquad (1)$$

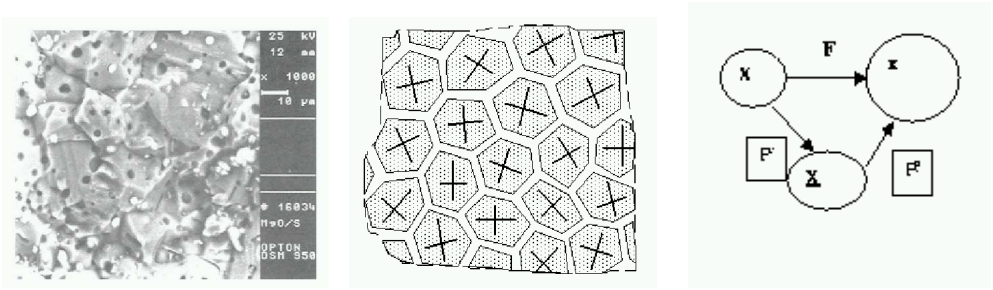

Figure 1: SME image (left), idealization (middle), gradient decomposition (right).

where $\mathbf{B}_{\mathrm{L}}^{\prime\mathrm{T}}$ is the large displacements operator, $\mathbf{B}_{\mathrm{L}}^{\mathrm{T}}$ is the linear operator, ${}_t^t\bar{\boldsymbol{\tau}}$ is the Cauchy stress matrix, $\Delta\mathbf{S}$ is the stress increment, $\mathbf{N}$ is the shape functions matrix, $\Delta\mathbf{q}$ is the displacements increment vector, $\Delta\mathbf{f}$ is the body forces increment vector and $\Delta\mathbf{t}$ is the tractions external load increment vector. When considering the finite strains effect[5,6] the

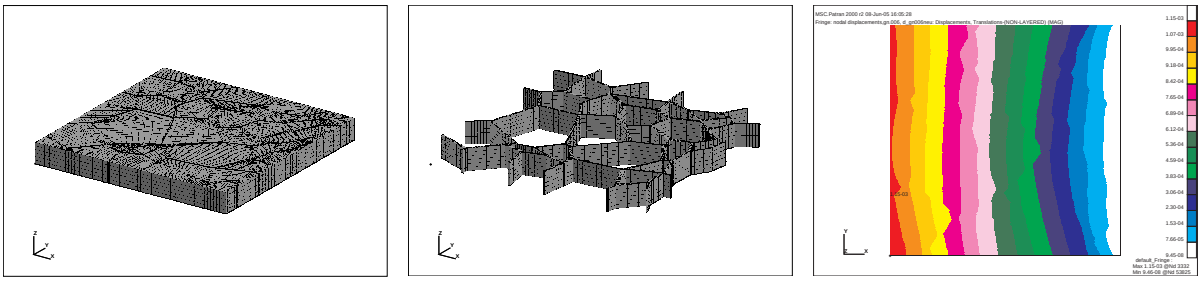

Figure 2: Discretization of RVE (left), interfaces (middle), displacement field before "first yield" (right).

gradient $\mathbf{F} = \partial(\mathbf{X} + \mathbf{u})\partial\mathbf{X}$ is decomposed into its elastic and plastic parts, $\mathbf{F} = \mathbf{F}^e\mathbf{F}^p$, Figure 1 (right). To integrate the constitutive relations the deformation increment $\Delta\mathbf{D}$ is rotated to the unrotated configuration by means of rotation matrix obtained from the polar decomposition $\mathbf{F} = \mathbf{VR} = \mathbf{RU}$, namely $\Delta\mathbf{d} = \mathbf{R}_{n+1}^{\mathrm{T}}\Delta\mathbf{D}\mathbf{R}_{n+1}$. Then, the radial return is performed and the stresses are transformed to the Cauchy stresses at $n+1$, namely $\sigma_{n+1} = \mathbf{R}_{n+1}\boldsymbol{\sigma}_{n+1}^{u}\mathbf{R}_{n+1}^{\mathrm{T}}$. The stresses are integrated using the consistent tangent formulation[7] and the integration is done in the unrotated configuration as for small strains.

3 NUMERICAL EXAMPLE

The mechanical properties of the polycrystal consisting of elastic grains and metallic interfaces are as follows; grains: Young modulus 4.1x10^{11}Pa and Poisson's ratio 0.25, interfaces: Young modulus 2.1x10^{11}Pa, Poisson's ratio 0.235, yield limit 2.97x10^{11}Pa and small hardening modulus 1.0x10^{6}Pa. The dimensions of the sample are 100x100x10 μm. The scheme of the Representative Volume Element is given in Figure 2 (left, middle). The RVE is discretized with 48894 elements and 58016 nodes. The sample is fixed on

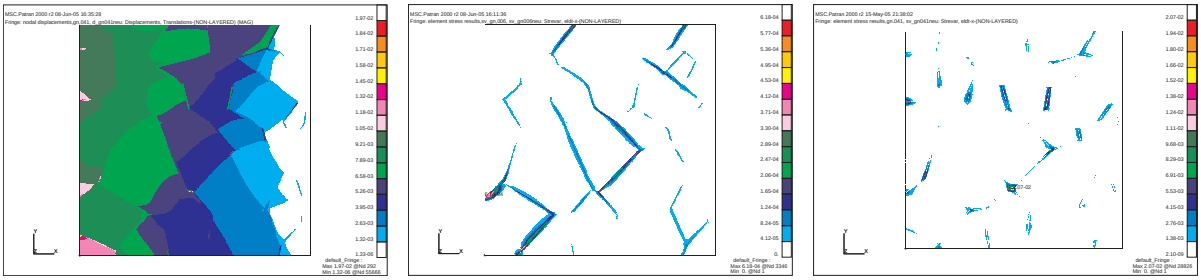

Figure 3: Displacement field before failure (left), equivalent plastic strains after first yield (middle) and and before failure (right).

one side and loaded with the uniform pressure of 400 MPa on the other one. There is imposed a symmetry condition in the bottom of the sample. Since the grains are elastic the sample fails due to large plastic strains occurring in the elasto-plastic interfaces. The displacement fields just before "first yield" and before failure are shown in Figure 2 (right) and in Figure 3 (left), respectively. There is demonstrated qualitative difference between

Figure 4: Spatial failure of the interfaces, axonometric view (left) and side view (middle), displacement vs load factor (right).

the two situations. The displacement field just before yielding exhibits discontinuities along interfaces (Figure 2, right). It can be interpreted that the grains tend to slide along the interfaces. Figure 3 (left) shows that the grains are strongly displaced and rotated. The failure is spatial (Figure 4, left and middle), namely, the ductile material of the interfaces is squeezed by the stiff grains and thrusted out of the sample. The crucial place appeared to be a very short segment of the interface parallel to the loading axis. The segment connects four other interfaces and is located between four grains. The equivalent plastic strains distributions just after "first yield" are shown in Figure 3 (middle) and before failure in Figure 3 (right). When comparing the Figures 3 middle and right we may notice that the distribution of equivalent plastic strains is qualitatively different after first yield and before failure. In the case of "first yield" (Figure 3, middle) the interfaces are getting plastic relatively uniformly and the already plastic interfaces

are arranged approximately in the angle of 45°. The situation is different before failure when the plastic strains are redistributed and strongly localized (Figure 3, right) close to connections of the interfaces. The highest plastic strains are in the interface segment corresponding to the one which is seen in Figure 4 (left, middle). This segment decides about the failure.

The load-displacement curves are presented in Figure 4 (right). A horizontal displacement along the load axis in the middle of the loaded face of the sample is chosen. We consider three cases: elasto-plastic (thick crosses), elasto-plastic and included geometrical imperfection (thin crosses), elasto-plastic and nonlinear geometry. A small geometric imperfection (void) is placed in the one of the interfaces in the middle of the sample. It can be noticed that when concerning this particular model the influence of the imperfection is not significant. The influence of the nonlinear geometry is important since it decides about the load carrying capacity of the sample. The load factor of the failure load is 4.0.

The communication presents the problem of failure load and failure mode of an RVE of a polycrystallic material. The most characteristic features of the failure mode are the grains rotations and spatial displacing of the interface material.

ACKNOWLEDGMENTS

The Author's would like to thank the Engineering and Physical Sciences Research Council (UK) for the support. The second Author has been supported by a Marie Curie Fellowship of the European Community.

REFERENCES

[1] O.C. Zienkiewicz and R.L. Taylor. *The finite element method*, Butterworth–Heinemann, 2000.

[2] D.R.J. Owen, E. Hinton. *Finite Elements in Plasticity*, Pineridge Press, 1980.

[3] K.J. Bathe. *Finite Element Procedures*, Prentice Hall, 1996.

[4] M. Kleiber. *Incremental finite element modelling in non-linear solid mechanics*, Polish Scientific Publishers, Ellis Horwood, 1989.

[5] P.M. Pinsky, M. Ortiz, K.S. Pister. Numerical integration of rate constitutive equations in finite deformations analysis, *Computer Methods in Applied Mechanics and Engineering*, **40**, 137–158, 1983.

[6] D. Peric, D.R.J. Owen, M.E. Honnor. A model for finite strain elasto-plasticity based on logarithmic strains: Computational issues, *Computer Methods in Applied Mechanics and Engineering*, **94**, 35–61, 1992.

[7] J.C. Simo, R.L. Taylor. Consistent tangent operators for rate independent elasto-plasticity, *Computer Methods in Applied Mechanics and Engineering*, **48**, 101–118, 1985.